ELECTROCHEMISTRY

Spin-induced asymmetry reaction—The formation of asymmetric carbon by electropolymerization

Deb Kumar Bhowmick[1], Tapan Kumar Das[1], Kakali Santra[1], Amit Kumar Mondal[1], Francesco Tassinari[1,2], Rony Schwarz[3], Charles E. Diesendruck[3], Ron Naaman[1]*

We describe the spin polarization–induced chirogenic electropolymerization of achiral 2-vinylpyridine, which forms a layer of enantioenhanced isotactic polymer on the electrode. The product formed is enantioenriched in asymmetric carbon polymer. To confirm the chirality of the polymer film formed on the electrode, we also measured its electron spin polarization properties as a function of its thickness. Two methods were used: First, spin polarization was measured by applying magnetic contact atomic force microscopy, and second, magnetoresistance was assessed in a sandwich-like four-point contact structure. We observed high spin-selective electron transmission, even for a layer thickness of 120 nm. A correlation exists between the change in the circular dichroism signal and the change in the spin polarization, as a function of thickness. The spin-filtering efficiency increases with temperature.

INTRODUCTION

The origin of chirality in life remains an exciting but still unresolved question (*1*). Recently, it has been suggested that the spin-polarized electrons could, in principle, provide a mechanism for initiating chirality (*2*). Here, we show that, starting from achiral molecules, a product with an asymmetric carbon can be formed, and this chirality is propagated through polymerization, resulting in continuous formation of enantioenhanced chiral groups in isotactic polymers.

Producing an enantiospecific chiral product from achiral reagents is an important goal in chemistry. This is typically achieved using enantiopure catalysts, such as enzymes, organometallic, or organocatalysts (*3*–*6*). In recent years, a new method to obtain asymmetric chiral products has been developed on the basis of the chiral-induced spin selectivity (CISS) effect (*7*). The CISS effect refers to the preferential transmission (or transfer) of electrons with one spin orientation over the other through chiral molecules. This effect was observed in redox reactions that involve the transfer of spin-polarized electrons (*8*–*11*). A magnetic catalyst has recently been used to make a product with asymmetric carbon when all the reactants are achiral (*12*).

To establish the new method, it is essential to determine to what extent the method is general and what mechanism controls enantioselectivity. To explore these issues, we investigated the spin-selective enantioenriched electropolymerization of 2-vinylpyridine. The electrons that are transmitted from the electrode through the newly formed radical anion maintain their spin polarization throughout propagation, even at higher degrees of polymerization. Hence, a mechanism for the efficient formation of chiral products is revealed.

Enantiopure chiral polymers have become an important component in chiral sensors (*13*, *14*). Chiral stationary phases, based on polymers, are also used in enantiomer separation and have found important applications in columns for chiral gas and high-performance liquid chromatography (HPLC) (*15*, *16*). In addition, polymers (*17*) and, more specifically, chiral polymers (*18*, *19*) are important materials for various spintronic applications (*20*). The results shown here provide inexpensive, general synthetic methods for producing chiral isotactic polymers from their achiral or racemic monomer units.

The electropolymerization of poly(2-vinyl pyridine) (PVP) is a well-established chemical process (*21*–*23*). The polymerization mechanism and its dependence on various ambient conditions have been studied extensively. The pH and the solvent combination play an essential role in polymer growth on the electrode surface. The quality of the polymer layer formed on solid substrates is higher when the layer is fabricated in acidic pH. Consequently, the layer grows uniformly on a solid substrate under a negative potential (*24*). Polymerization occurs through protonation, followed by electron transfer from the cathode to the monomer unit, forming a radical, as shown in Fig. 1A (*25*). This radical propagates through reaction with another monomer, forming a dimer and so on. Termination typically occurs through recombination or oxidation. In electropolymerization, over time, continuous termination and new initiations occur, even on the top of the previous present chains. This results in the formation of thick, multilayer polymer coatings on the working electrode.

PVP consists of an aliphatic backbone with pyridyl substitutes. Consequently, every second carbon atom in the backbone is stereogenic. Addition of each monomer unit to the growing polymer backbone creates a new chiral center. Here, we show that the electron's spin polarization controls the chirality through the polymer chain propagation. The spin polarization is defined by the direction of the magnetization of the ferromagnetic working electrode. Each spin state produces a different enantiomer. Hence, the chirality of the final isotactic polymer can be simply controlled (see Fig. 1B).

RESULTS

The PVP layers were electrochemically grown on ferromagnetic solid surfaces (gold-coated Ni surfaces) magnetized perpendicular to the surface, with the north magnetic pole pointing either toward the solution (up) or away from the solution (down). For control experiments, an unmagnetized surface was used. An argon saturated solution of 0.25 M of 2-vinylpyridine in 9:1 water-methanol (0.25 M) at pH 4.8 was used to grow the polymer layers on the solid surface. Ammonium perchlorate was used as an electrolyte. Various

[1]Department of Chemical and Biological Physics, Weizmann Institute, Rehovot 7610001, Israel. [2]Department of Chemical and Geological Sciences, University of Modena and Reggio Emilia, Via Campi 103, 41125 Modena, Italy. [3]Schulich Faculty of Chemistry, Technion, Israel Institute of Technology, Haifa, 3200008 Israel.
*Corresponding author. Email: ron.naaman@weizmann.ac.il

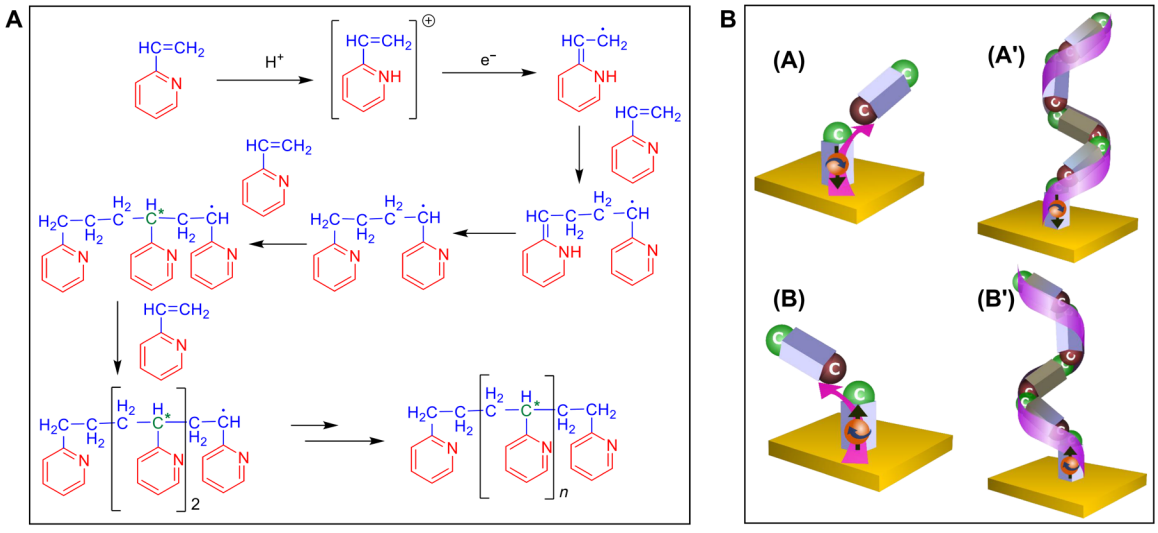

Fig. 1. Schematic and a proposed mechanism of the electropolymerization process of 2-vinylpyridine. (**A**) Schematic of the electropolymerization process of 2-vinylpyridine (*25*). (**B**) Schematic of a proposed mechanism for enantioselective polymerization in the presence of spin-polarized electrons. After the adsorption of the first monomer on the electrode (yellow), a second monomer is adsorbed either in the pro–right-handed (A) or in the pro–left-handed (B) configuration. Spin-polarized electrons are transferred from the electrode into the complex formed. Which spin polarization is injected depends on the magnetization direction of the substrate. One spin-polarized electron (the sphere with an arrow) is preferred for the right-handed configuration, and the opposite spin is preferentially transferred for the left-handed structure. The asymmetric carbon is denoted in green. The sequential polymerization continues, and accordingly, either right-handed (A') or left-handed structures (B') are formed. No evidence for the secondary structure of the polymer could be obtained.

thicknesses of polymer layers were produced chronoamperometrically for different times by applying a constant potential of −1.2 V (*24*). The polymer layers' thicknesses were monitored using polarization-modulated infrared reflection absorption spectroscopy (PMIRRAS) and atomic force microscopy (AFM) measurements. The chiral nature of the polymer layers was determined using circular dichroism (CD) measurements. Specifically, the CD spectra of the short polymers (after 5 min of polymerization) were also measured (fig. S3E), and the existence of asymmetric carbon chirality was verified.

The polymerization products were analyzed using proton nuclear magnetic resonance (NMR), matrix-assisted laser desorption/ionization–time-of-flight (MALDI-TOF) mass measurements, and size exclusion chromatography (SEC). A typical NMR spectrum is shown in fig. S10. The spectrum of PVP was obtained from the electropolymerization of 2-vinylpyridine on a Ni-Au surface for 5 min. The proton signals at δ = 8.5 and 7.8 to 6.8 parts per million (ppm) correspond to the aromatic protons from the pyridine ring. In contrast, broad signals between δ = 2.2 and 0.5 ppm correspond to the methine and methylene groups at the polymer's backbone. In the ^{1}H-NMR signals of the monomer 2-vinylpyridine (fig. S11), four aromatic protons appear at δ = 8.45 and at 7.45, 7.16, and 6.8 ppm, and three alkene protons appear at 6.7, 6.1, and 5.34 ppm. The broad nature of the proton signals of the electropolymerized product is due to the presence of metal ions that are incorporated during the collection of product from metal surfaces. Polymerization can be confirmed by the absence of alkene proton signals, which are present in the vinyl pyridine monomer. Deconvolution of the pyridine H-6 proton signal (fig. S12) indicates around 50% tacticity of the chiral polymer grown for 5 min in the case of north magnetic pole–pointing condition.

The MALDI mass spectra were measured for four PVPs samples grown on the electrode for different times (fig. S13). The average mass [mass/charge ratio (*m*/*z*)] of the polymer increases slightly from 689.2 to 948.4 when the reaction time changes from 2 to 7 min. For the polymer layer grown for 5 min, the mass distributions of the polymer (*m*/*z*) are shown between 627.9 and 2322.0, which correspond to chains of approximately 6 to 22 monomer units, with the strongest signal for the chain with 8 monomer units.

MALDI-TOF is known to provide higher-intensity signals for lower–molecular weight oligomers, and therefore, SEC of the isolated electropolymerized materials after different reaction times was obtained. The oligomers were obtained by washing the surfaces with acetonitrile, followed by evaporation and dissolution in HPLC-grade *N*,*N*′-dimethylformamide (DMF). DMF-SEC-MALS (multi-angle light scattering) at 50°C was performed, providing precise molecular weights and polydispersities (table S1). The main polymer peak shifts to shorter retention times as the polymerization time increases, supporting the increase in the average molecular weight, as shown in fig. S4. The calculated molecular weights indicate the presence of polymers having several tens of monomers per chain. Moreover, a higher–molecular weight peak appears with twice the molecular weight of the main peak, supporting radical recombination as a termination mechanism.

The PMIRRAS measurements focused on the C-H stretching region. Figure S5A presents the infrared (IR) spectra of polymer-coated surfaces grown at different time periods and monomer-coated surfaces. The IR spectra of the electropolymerized surfaces show the clear abundance of the methylene C-H stretching bands at 2858 and 2927 cm^{-1} in the polymer backbone because of C-H symmetric and antisymmetric stretching, respectively. C-H peaks at 3007 and 3059 cm^{-1} originate from the pyridine group present in the polymer side chain. For the monomer-coated surface, along with methylene and pyridine C-H stretching signals, alkene C-H stretching band at 3026 cm^{-1} is also present. The absence of alkene C-H stretching band in the

polymer-coated surfaces and the presence of methylene signals confirm the successful formation of the polymer coating on the solid surfaces. Partial polymerization of the monomer-coated surface during drying at room temperature causes the appearance of a weak methylene signal. Figure S5A shows a gradual increase in the characteristic signal intensities as the polymer growth time increases. This indicates that the thickness of the polymer layer can be controlled by varying the reaction time.

The AFM images provide detailed information on the shape of the polymer layers and their thicknesses on the paramagnetic substrates. Figure S5B shows the AFM topography image for a polymer layer deposited for 3 min on a gold-coated nickel surface. The AFM image suggests the formation of a compact polymer layer on the substrate. Some pinholes can be recognized because of trapped hydrogen bubbles at the working electrode, which are formed during the polymerization process. Because polymerization had been carried out at a potential of −1.2 V, a parallel H_2O splitting reaction took place, producing H_2 gas at the working electrode. The line profile along the surface (fig. S5C) indicates a polymer thickness of about 60 nm. Thicknesses of polymers grown for different times are determined similarly. Table S2 shows the layer thickness for polymers grown for 2 to 7 min, with the thickness varying from 20 to 120 nm.

CD measurements were conducted on the polymer layers adsorbed on quartz coated with 5 nm of Ti, 15 nm of Ni, and 5 nm of Au. Polymerizations were performed using these substrates as working electrodes in the presence of the north pole of the magnetic field of the substrate pointing toward the electrolyte solution (up) or away from it (down) or with no magnetic field. The obtained CD spectra are shown in Fig. 2, and the corresponding ultraviolet absorption spectra are shown in fig. S3. Polymers grown on the ferromagnetic substrate with the north pole pointing down (D-polymer) show positive CD values. In contrast, those grown with the north pole pointing up (L-polymer) show negative CD values (Fig. 2, A and B, respectively). These signals fit well with previous studies on isotactic PVP prepared using stereoselective polymerization, but in the present study, both the nature of the chiral centers present in the backbone and the secondary structure of the polymer are a consequence of the spin polarization of the electrons (*26*). The CD spectra of a short oligomer chain of about six monomer units in methanol (fig. S3E) show opposite CD signals when prepared in the presence of the north magnetic pole pointing up and down. The shape of the CD signal is similar to the enantiopure isotactic PVP, as shown in (*27*). The polymer chain length is too short to form a helical structure in solution state without the addition of any secondary salt. Hence, the CD signal can only be explained by the presence of enantioenriched static chirality in the polymer. Two opposite magnetic poles influenced the formation of two opposite enantioenriched chiral polymer products. Figure 2 (C and D) shows the change in the CD and the Δg values, respectively, with polymerization progress. Initially, a sharp linear increase in CD signal is observed until 3 min of polymerization, with further polymerization resulting in a slower change in the CD signal. This trend is similar for both the L- and D-polymers. The change in the slope is a result from the multiple polymer layer formation, which reduces the spin polarization, which will be discussed below. A reduction in the enantioselectivity as a function of thickness is also evident from the reduction in Δg values (see the Supplementary Materials for the detailed calculation). The slight asymmetry in the intensity of the CD signals for the L- and D-polymers may arise from a small difference in the effective area of the electrodes or from their slightly different surface roughness. The polymer layer grown in the absence of a magnetic field shows no CD signal (fig. S3C), which corresponds to the racemic polymer layer formation on the solid surface.

Two measurement techniques, magnetoresistance (MR) and magnetic conductive AFM (mc-AFM), were used to determine the CISS effect of the polymer-coated surfaces at different polymerization times. The aims of these measurements were to demonstrate spin selectivity even in thicker polymer films and to demonstrate that spin selectivity increases even after the polymer layer is tens of nanometers thick. The differences between the MR and mc-AFM methods and the relationship between the chiral structure of molecules and the spin-filtering properties were established in numerous studies, and a qualitative model was recently presented (*28*).

The MR of the devices made with the polymer were measured using a four-probe configuration with crossbar geometry. These measurements provide insight into temperature-dependent spin transport through the polymers. A schematic representation of the device is shown in Fig. 3A (*29*). The MR is defined as MR (%) = $\frac{(R_H - R_{H=0})}{(R_{H=0})} \times 100$, where $R_{H=0}$ and R_H are the zero-field and zero-infield resistance, respectively. MR was measured on all polymer-coated surfaces prepared under different conditions. Figure 3 (B and C) shows the MR spectra of the PVP layers grown for 3 and 5 min when the substrate was magnetized with the north pole of the magnetic field pointing either up or down. The spectra were collected as a function of the magnetic field between −1.0 and 1.0 T at different temperatures. The curves exhibit an asymmetric nature as a function of the magnetic field, as observed in previous studies for chiral molecular systems (*30*). This confirms the opposite chirality of polymers grown in the presence of opposite spin-polarized electrons. The spectra show about 2% MR at 250 K for both handednesses. The low MR values may be caused by the random distribution of polymers on solid surfaces, leading to the production of many pinholes from trapped H_2 bubbles on the surface during polymerization. The current can flow directly through these pinholes without passing through the chiral medium.

Figure 3D presents the MR values at 250 K for polymer layers of different thicknesses. The red and blue lines denote the polymer layers grown with the north pole pointing either up (L) or down (D). In both cases, the MR increases until a certain thickness and then decreases. We attribute the decrease in the MR to the random alignment of the polymer structure after a certain thickness. This random structure enhances the electron scattering and, hence, the spin randomization. Figure 3E presents the temperature-dependent MR values of the two best systems of L-polymer (red) and D-polymer (blue). The MR values increase with increased temperature. The overall MR values obtained for the L-polymer are higher than those in the D-polymer; this corresponds to a similar observation in the CD measurements.

mc-AFM measurements were performed to study the spin selectivity of electrons transmitted through the polymer films (*31*). Figure 4A presents a schematic of an mc-AFM setup; by varying the direction of the magnetic field of the ferromagnetic substrate, it is possible to measure the spin-dependent current through the interface at different voltages. The AFM tip restricts the interface's contact area; therefore, it is possible to obtain current-voltage relation (*I-V*) curves for a nanometer-scale area. This overcomes the difficulties due to interface defects. Polymers coated on nickel-gold surfaces (Au/Ni) were used in these measurements. During the measurements,

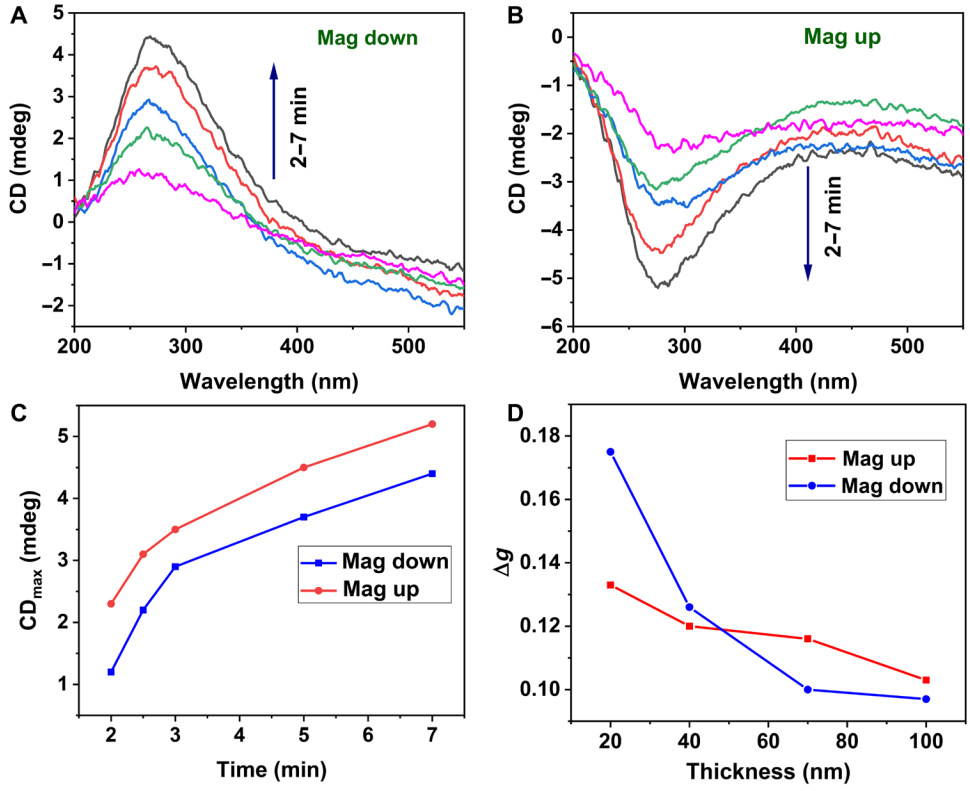

Fig. 2. CD results of PVP layer on Ni-Au–coated quartz substrate. CD spectra measured at various time intervals from 2 to 7 min during the electropolymerization of 2-vinylpyridine in the presence of the north magnetic pole of the Ni-Au–coated quartz substrate pointing away from the solution (Mag down) (**A**) and toward the solution (Mag up) (**B**). (**C**) The change in the CD_{max} values during polymerization as a function of polymerization time. (**D**) The change in the *g* factor as a function of the thickness of the polymer layer. Mag, magnet.

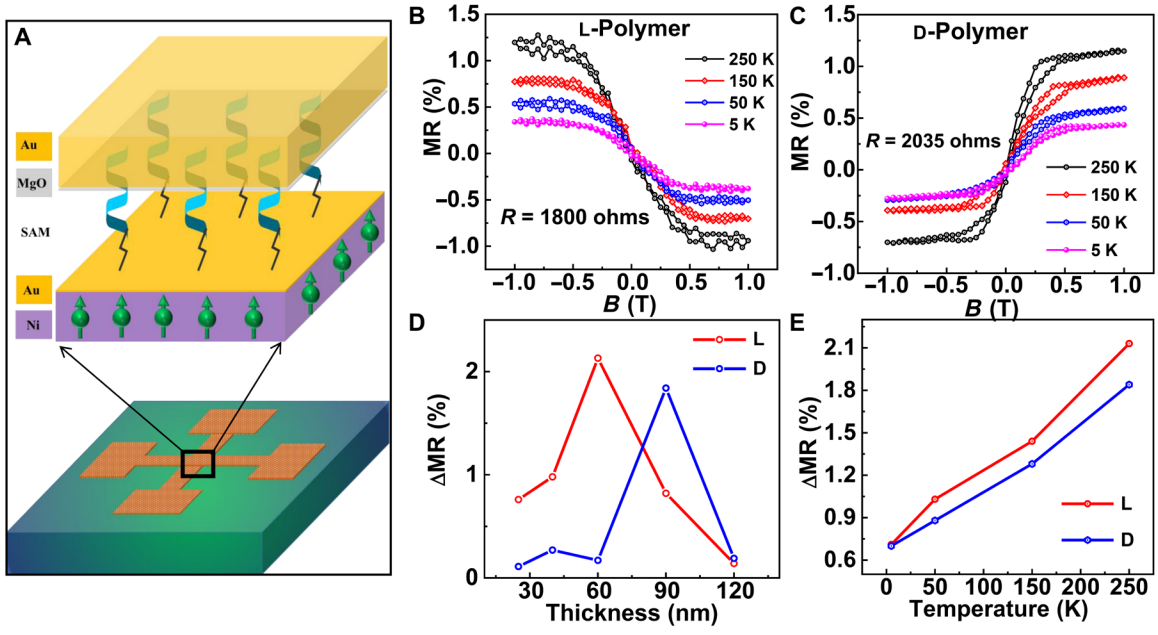

Fig. 3. Temperature-dependent MR studies. (**A**) Schematic representation of the four-probe MR measurement setup, with the bottom Ni-gold and top gold electrode. (**B** and **C**) MR curves for films obtained from L-polymer and D-polymer, respectively, as a function of a magnetic field between −1.0 and 1.0 T at different temperatures. (**D**) The dependence of MR on the thickness of the polymer layers synthesized when the north pole of the magnet substrate points up (L-polymer) or down (D-polymer). The measurements were performed at a constant current of 0.5 mA. (**E**) Normalized ΔMR values as a function of temperature, where $\Delta MR\ (\%) = |MR\ (\%)|_{-1.0T} + |MR\ (\%)|_{+1.0T}$.

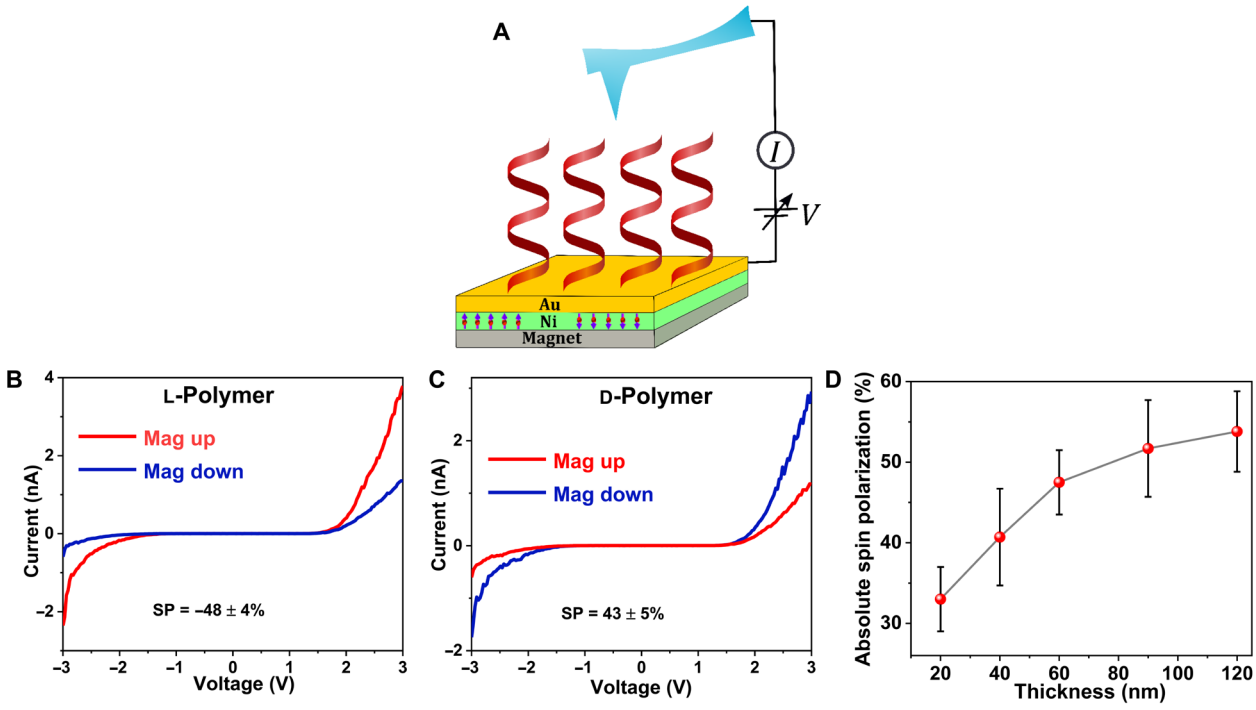

Fig. 4. Spin polarization measured with mc-AFM. (**A**) Schematic representation of the mc-AFM setup. (**B** and **C**) Average *I-V* curves recorded for polymers synthesized in magnet up (L-polymer) and down directions (D-polymer). The red and blue lines denote the average *I-V* curves with the magnet's north pole pointing in the up and down directions, respectively. The sample's thickness in all the measurements was 60 ± 3 nm. (**D**) The dependence of the spin polarization (the absolute value) on the thickness of the layers of polymers synthesized in the magnet up direction.

the AFM tip remains grounded, while the substrate's potential varies from −3 to +3 V. The current is measured perpendicular relative to the substrate's surface. Figure 4 (B and C) shows the current as a function of applied potential when the magnetic electrode was magnetized with either the north or south magnetic pole pointing up.

Regarding the L-polymer, a higher current was observed when the measurement was carried out with the substrate magnetization with the north magnetic pole facing up compared to it pointing down (Fig. 4B). However, the opposite behavior was observed for the D-polymer; here, a higher current was observed when the north magnetic pole was pointing down (Fig. 4C). All results show the nonlinear dependence of the current on the applied voltage. Different threshold potentials for charge injection are observed for the two spin states, indicating that no spin flipping occurs during the electron transmission (*32*). From the current versus voltage curves of the two spin states, it is possible to calculate the spin polarization, SP (%) $= \frac{I_{down} - I_{up}}{I_{up} + I_{down}} \times 100$, at a particular applied potential, where I_{up} and I_{down} are the currents measured when the north magnetic pole is pointing toward and away from the substrate, respectively. The data from Fig. 4B result in an average spin polarization of about −48 ± 4% for the L-polymer, and based on Fig. 4C, the spin polarization is 43 ± 5% for the D-polymers, and the polymer thickness is about 60 nm. The spin polarization as a function of the polymer thickness for the L-polymer is presented in Fig. 4D.

DISCUSSION

The spin polarization increases with an increase in the layer thickness. Initially, the spin polarization increases rapidly, to a thickness of about 60 nm; however, the increase is more moderate for thicker films. A very similar trend is observed in the CD signals with respect to layer thicknesses, as shown in Fig. 2C. Hence, the spin polarization is proportional to the optical activity of the films. Namely, until a thickness of 60 nm is reached, both the CD signal and the spin polarization increase linearly with the length. With further increases in layer thickness (along with further increases in the polymerization time), the changes are more gradual. The correlation between the polymer's CD signal and the spin polarization in the CISS effect was also observed in previous studies (*33*, *34*). The correlation between the change in spin polarization and the change in the CD signal supports the mechanism underlying spin polarization–controlled enantioselective polymerization. Namely, if the enantioselectivity would result from the formation of a chiral layer on the electrode only, then there is no reason to expect that the growth in the CD would decrease as a function of the layer thickness.

The long-range spin transport observed is consistent with former observations that indicate that spin polarization can be observed even after electrons are conducted through hundreds of nanometers of chiral materials (*35*–*38*). However, the present results are the first long-range spin transport observed in noncrystallinic polymers, suggesting that the process studied here can be used for efficiently obtaining large amounts of chiral products.

Because polymerization, described here, is a radical chain reaction, the spin-polarized radical at the electrode surface controls the conformation of the asymmetric carbon center, which is generated by adding monomer units. Namely, in the electropolymerization process, when one monomer is in contact with the magnetized substrate and another monomer approaches the adsorbed one, the spin-polarized electron passes from the substrate through the first monomer into the interaction region with the second monomer, as

shown in Fig. 1B. In principle, the two monomers together can form a temporary complex having either a left-handed or right-handed chiral symmetry. Because of the CISS effect, the spin-polarized electron will penetrate easier into a complex having a symmetry that fits the conduction of its spin. Hence, a reaction will be promoted mainly for dimers that have a specific handedness. This process repeats itself throughout propagation.

The process of forming a chiral polymer from an achiral reagent without a chiral catalyst demonstrates the power of spin-induced enantiospecific chemistry. The material obtained has interesting spintronic properties at room temperature; hence, it has the ability to produce new organic spintronic devices and applications.

MATERIALS AND METHODS

Reagents

2-Vinylpyridine (97%), ammonium perchlorate (99.5%), and perchloric acid (99.99%) were purchased from Sigma-Aldrich Merck. Reagent-grade ultrapure water (nuclease Free) was purchased from Hylabs.

Substrates

Quartz wafers (0.5 mm thick), silicon (100) (resistivity, 0.001 to 0.005 ohm cm) wafers, and 3000-Å-thick thermally grown silicon oxide on Si (100) wafers were purchased from Micquartz, UniversityWafer, and Silicon Valley Microelectronics, respectively. For the polymerization experiments, four types of substrates were prepared. For CD measurements, 8 nm of Ti, 15 nm of Ni, and 5 nm of Au were deposited on quartz substrates. In addition, 8 nm of Ti, 80 nm of Ni, and 7 nm of Au layers on Si (100) substrates were used for the magnetic AFM measurements. Substrates for MR were prepared by depositing 8 nm of Ti, 30 nm of Au, 25 nm of Ni, and 5 nm of Au on 3000-Å thermal oxide-grown Si (100) wafers using a mask with line structures of 50 μm width and 3 mm length. Substrates of 8 nm of Ti and 100 nm of Au on Si (100) were used for the PMIRRAS measurements.

Electrochemistry

All electrochemical measurements were performed with a PalmSens4 potentiostat using PSTrace software. For our experiments, a three-electrode configuration was used. Ag/AgCl (s) with a saturated KCl solution and a platinum wire were used as reference and counter electrodes, respectively. Nickel-gold–coated surfaces were used as working electrodes. A solution of 0.25 M 2-vinylpyridine and 0.05 M NH_4ClO_4 in a 9:1 water-methanol mixture at pH 4.8 was used for electropolymerization. The pH of the reaction mixture was adjusted to pH 5 by adding perchloric acid. The methanol and water were degassed with Ar before preparing the solution for electropolymerization. For the cyclic voltammetry measurements, the potential was swept twice between −0.7 and −1.8 V with respect to Ag/AgCl and with a scan rate of 0.2 V/s. Chronoamperometry was measured at a constant potential of −1.2 V.

SUPPLEMENTARY MATERIALS

Supplementary material for this article is available at https://science.org/doi/10.1126/sciadv.abq2727

REFERENCES AND NOTES

1. M. Frenkel-Pinter, M. Samanta, G. Ashkenasy, L. J. Leman, Prebiotic peptides: Molecular hubs in the origin of life. *Chem. Rev.* **120**, 4707–4765 (2020).
2. R. A. Rosenberg, Electrochirogenesis: The possible role of low-energy spin-polarized electrons in creating homochirality. *Symmetry* **11**, 528 (2019).
3. R. E. Gawley, J. Aube, *Principles of Asymmetric Synthesis: Volume 14, Tetrahedron Organic Chemistry* (Elsevier Science & Technology, 2004).
4. D. R. Boyd, M. A. Mckervey, Asymmetric synthesis. *Q. Rev. Chem. Soc.* **22**, 95–122 (1968).
5. M. Hideto, T. Yoshiji, Discovery and application of asymmetric reaction by multifunctional thioureas. *Bull. Chem. Soc. Jpn.* **81**, 785–795 (2008).
6. H. M. L. Davies, Q. Jin, Catalytic asymmetric reactions for organic synthesis: The combined C H activation/Cope rearrangement. *Proc. Natl. Acad. Sci. U.S.A.* **101**, 5472–5475 (2004).
7. D. H. Waldeck, R. Naaman, Y. Paltiel, The spin selectivity effect in chiral materials. *APL Mater.* **9**, 040902 (2021).
8. T. S. Metzger, S. Mishra, B. P. Bloom, N. Goren, A. Neubauer, G. Shmul, J. Wei, S. Yochelis, F. Tassinari, C. Fontanesi, D. H. Waldeck, Y. Paltiel, R. Naaman, The electron spin as a chiral reagent. *Angew. Chem. Int. Ed. Engl.* **59**, 1653–1658 (2020).
9. B. P. Bloom, Y. Lu, T. Metzger, S. Yochelis, Y. Paltiel, C. Fontanesi, S. Mishra, F. Tassinari, R. Naaman, D. H. Waldeck, Asymmetric reactions induced by electron spin polarization. *Phys. Chem. Chem. Phys.* **22**, 21570–21582 (2020).
10. F. Tassinari, D. Amsallem, B. P. Bloom, Y. Lu, A. Bedi, D. H. Waldeck, O. Gidron, R. Naaman, Spin-dependent enantioselective electropolymerization. *J. Phys. Chem. C* **124**, 20974–20980 (2020).
11. R. Naaman, Y. Paltiel, D. H. Waldeck, Chiral induced spin selectivity gives a new twist on spin-control in chemistry. *Acc. Chem. Res.* **53**, 2659–2667 (2020).
12. T. S. Metzger, R. Siam, Y. Kolodny, N. Goren, N. Sukenik, S. Yochelis, R. Abu-Reziq, D. Avnir, Y. Paltiel, Dynamic spin-controlled enantioselective catalytic chiral reactions. *J. Phys. Chem. Lett.* **12**, 5469–5472 (2021).
13. G. Fukuhara, Polymer-based supramolecular sensing and application to chiral photochemistry. *Polym. J.* **47**, 649–655 (2015).
14. X. Shang, I. Song, G. Y. Jung, W. Choi, H. Ohtsu, J. H. Lee, J. Y. Koo, B. Liu, J. Ahn, M. Kawano, S. K. Kwak, J. H. Oh, Chiral self-sorted multifunctional supramolecular biocoordination polymers and their applications in sensors. *Nat. Commun.* **9**, 3933 (2018).
15. E. Yashima, Polysaccharide-based chiral stationary phases for high-performance liquid chromatographic enantioseparation. *J. Chromatogr. A* **906**, 105–125 (2001).
16. D. D. Medina, Y. Mastai, Chiral polymers and polymeric particles for enantioselective crystallization. *Isr. J. Chem.* **58**, 1330–1337 (2018).
17. P. Bujak, I. Kulszewicz-Bajer, M. Zagorska, V. Maurel, I. Wielgus, A. Pron, Polymers for electronics and spintronics. *Chem. Soc. Rev.* **42**, 8895–8999 (2013).
18. P. C. Mondal, N. Kantor-Uriel, S. P. Mathew, F. Tassinari, C. Fontanesi, R. Naaman, Chiral conductive polymers as spin filters. *Adv. Mat.* **27**, 1924–1927 (2015).
19. D. Di Nuzzo, C. Kulkarni, B. Zhao, E. Smolinsky, F. Tassinari, S. C. J. Meskers, R. Naaman, E. W. Meijer, R. H. Friend, High circular polarization of electroluminescence achieved via self-assembly of a light-emitting chiral conjugated polymer into multidomain cholesteric films. *ACS Nano* **11**, 12713–12722 (2017).
20. J. Wade, J. N. Hilfiker, J. R. Brandt, L. Liirò-Peluso, L. Wan, X. Shi, F. Salerno, S. T. J. Ryan, S. Schöche, O. Arteaga, T. Jávorfi, G. Siligardi, C. Wang, D. B. Amabilino, P. H. Beton, A. J. Campbell, M. J. Fuchter, Natural optical activity as the origin of the large chiroptical properties in π-conjugated polymer thin films. *Nat. Commun.* **11**, 6137 (2020).
21. A. De Bruyne, J. -L. Delplancke, R. Winand, Electropolymerization of poly(2-vinylpyridine) films on zinc. *J. Appl. Electrochem.* **25**, 284–290 (1995).
22. X. Ling, M. D. Pritzker, C. M. Burns, J. J. Byerley, Effects of reaction conditions on the formation of poly(2-vinylpyridine) coatings by electropolymerization. *J. Coat. Technol.* **72**, 71–80 (2000).
23. H. Nakano, Y. Kuwahara, S. Oue, S. Kobayashi, H. Fukushima, J.-M. Yoon, Formation of poly(2-vinylpyridine) films on Zn by galvanostatic electropolymerization. *Mater. Trans.* **46**, 281–286 (2005).
24. X. Ling, J. J. Byerley, M. D. Pritzker, C. M. Burns, Critical effect of pH on the formation of organic coatings on mild steel by the aqueous electropolymerization of 2-vinylpyridine. *J. Appl. Electrochem.* **27**, 1343–1348 (1997).
25. X. Ling, M. D. Pritzker, C. M. Burns, J. J. Byerley, A mechanism for electropolymerization of 2-vinylpyridine coatings on metal surfaces. *Macromolecules* **31**, 9134–9140 (1998).
26. L.-C. Chen, Y.-C. Mao, S.-C. Lin, M.-C. Li, R.-M. Ho, J.-C. Tsai, Induced circular dichroism of stereoregular vinyl polymers. *Chem. Commun.* **48**, 3668–3670 (2012).
27. T. Wen, H.-F. Wang, Y.-C. Mao, W.-T. Chuang, J.-C. Tsai, R.-M. Ho, Directed crystallization of isotactic poly(2-vinylpyridine) for preferred lamellar twisting by chiral dopants. *Polymer* **107**, 44–53 (2016).
28. T. K. Das, F. Tassinari, R. Naaman, J. Fransson, Temperature-dependent chiral-induced spin selectivity effect: Experiments and theory. *J. Phys. Chem. C* **126**, 3257–3264 (2022).
29. S. P. Mathew, P. C. Mondal, H. Moshe, Y. Mastai, R. Naaman, Non-magnetic organic/inorganic spin injector at room temperature. *Appl. Phys. Lett.* **105**, 242408 (2014).
30. K. Michaeli, V. Varade, R. Naaman, D. Waldeck, A new approach towards spintronics–spintronics with no magnets. *J. Phys. Condens. Matter* **29**, 103002 (2017).

31. S. Mishra, A. K. Mondal, E. Z. B. Smolinsky, R. Naaman, K. Maeda, T. Nishimura, T. Taniguchi, T. Yoshida, K. Takayama, E. Yashima, Spin filtering along chiral polymers. *Angew. Chem. Int. Ed.* **59**, 14671–14676 (2020).
32. S. Mishra, A. K. Mondal, S. Pal, T. K. Das, E. Z. B. Smolinsky, G. Siligardi, R. Naaman, Length-dependent electron spin polarization in oligopeptides and DNA. *J. Phys. Chem. C* **124**, 10776–10782 (2020).
33. B. P. Bloom, B. M. Graff, S. Ghosh, D. N. Beratan, D. H. Waldeck, Chirality control of electron transfer in quantum dot assemblies. *J. Am. Chem. Soc.* **139**, 9038–9043 (2017).
34. A. K. Mondal, M. D. Preuss, M. L. Ślęczkowski, T. K. Das, G. Vantomme, E. W. Meijer, R. Naaman, Spin filtering in supramolecular polymers assembled from achiral monomers mediated by chiral solvents. *J. Am. Chem. Soc.* **143**, 7189–7195 (2021).
35. A. K. Mondal, N. Brown, S. Mishra, P. Makam, D. Wing, S. Gilead, Y. Wiesenfeld, G. Leitus, L. J. W. Shimon, R. Carmieli, D. Ehre, G. Kamieniarz, J. Fransson, O. Hod, L. Kronik, E. Gazit, R. Naaman, Long-range spin-selective transport in chiral metal–organic crystals with temperature-activated magnetization. *ACS Nano* **14**, 16624–16633 (2020).
36. Y.-H. Kim, Y. Zhai, H. Lu, X. Pan, C. Xiao, E. A. Gaulding, S. P. Harvey, J. J. Berry, Z. V. Vardeny, J. M. Luther, M. C. Beard, Chiral-induced spin selectivity enables a room-temperature spin light-emitting diode. *Science* **371**, 1129–1133 (2021).
37. H. Lu, C. Xiao, R. Song, T. Li, A. E. Maughan, A. Levin, R. Brunecky, J. J. Berry, D. B. Mitzi, V. Blum, M. C. Beard, Highly distorted chiral two-dimensional tin iodide perovskites for spin polarized charge transport. *J. Am. Chem. Soc.* **142**, 13030–13040 (2020).
38. K. Shiota, A. Inui, Y. Hosaka, R. Amano, Y. Ōnuki, M. Hedo, T. Nakama, D. Hirobe, J.-i. Ohe, J.-i. Kishine, H. M. Yamamoto, H. Shishido, Y. Togawa, Chirality-induced spin polarization over macroscopic distances in chiral disilicide crystals. *Phys. Rev. Lett.* **127**, 126602 (2021).
39. N. Berova, L. Di Bari, G. Pescitelli, Application of electronic circular dichroism in configurational and conformational analysis of organic compounds. *Chem. Soc. Rev.* **36**, 914–931 (2007).
40. A. Dworak, W. J. Freeman, H. J. Harwood, Epimerization and NMR spectra of poly(2-vinylpyridine). *Polym. J.* **17**, 351–361 (1985).

Acknowledgments

Funding: We acknowledge the support of the Israel Ministry of Science and the U.S. Department of Energy (grant no. ER46430). **Author contributions:** D.K.B. conceived the idea and performed studies. T.K.D. performed the MR studies. K.S. measured the CD spectra. A.K.M. performed the AFM studies. F.T. helped in designing the electrochemical system and in analyzing the data. R.S. and C.E.D. performed the GPC and were involved in writing the manuscript. R.N. designed the measurements and wrote the manuscript. **Competing interests:** R.N. and F.T. are inventors on a provisional patent application related to this work filed by Yeda Ltd. (Weizmann Institute) (no. 62/749,271, filed 23 October 2018). R.N. and F.T. are inventors on a provisional patent application related to this work filed by Yeda Ltd. (Weizmann Institute) and Yissum Ltd. (Hebrew University) (no. 62/749,271, filed 23 October 2019). The authors declare that they have no other competing interests. **Data and materials availability:** All data needed to evaluate the conclusions in the paper are present in the paper and/or the Supplementary Materials.

Submitted 29 March 2022
Accepted 27 June 2022
Published 10 August 2022
10.1126/sciadv.abq2727

ScienceAdvances

Spin-induced asymmetry reaction—The formation of asymmetric carbon by electropolymerization

Deb Kumar BhowmickTapan Kumar DasKakali SantraAmit Kumar MondalFrancesco TassinariRony SchwarzCharles E. DiesendruckRon Naaman

Sci. Adv., 8 (31), eabq2727. • DOI: 10.1126/sciadv.abq2727

Science Advances (ISSN) is published by the American Association for the Advancement of Science. 1200 New York Avenue NW, Washington, DC 20005. The title *Science Advances* is a registered trademark of AAAS.